Nitrogen trapping as a therapeutic strategy in tumors with mitochondrial dysfunction

Madala et al.

Supplemental Information:

Supplementary Figure S1 – S18

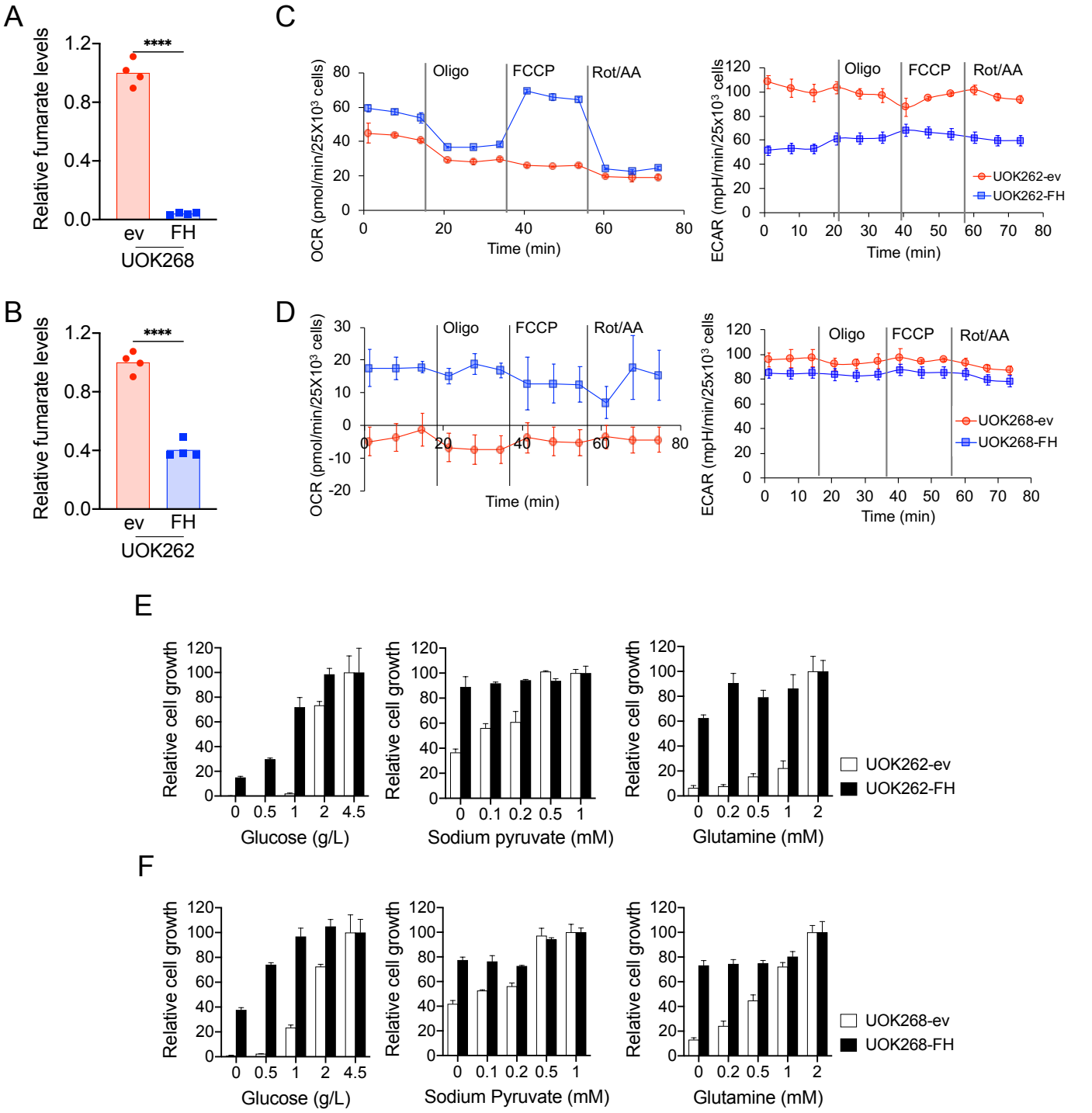

Figure S1. Characterization of UOK262, UOK268 and their FH-replete cell pairs.

(A-B) Mass spectrometry analysis of UOK262 and UOK268 cell pairs shows decreased fumarate levels upon introduction of wild-type FH into UOK262 and UOK268 cells. Data are shown as mean and individual data points (unpaired Student t test, ****P ≤ 0.0001).

(C-D) Extracellular flux analysis from Seahorse XF Cell Mito Stress Assay of UOK262 and UOK268 cell pair shows changes in the mitochondrial (left) and glycolytic (right) metabolism upon introduction of wild-type FH into UOK262 or UOK268 cells (mean ± SD, n = 4). OCR, oxygen consumption rate; ECAR, extracellular acidification rate.

(E-F) The *in vitro* growth of UOK262 and UOK268 as measured with the CellTiter-Glo assay indicating reduced dependency on glucose, pyruvate and glutamine upon repleting wild-type FH (mean ± SD, n = 3).

ev, empty vector; FH, wild-type FH.

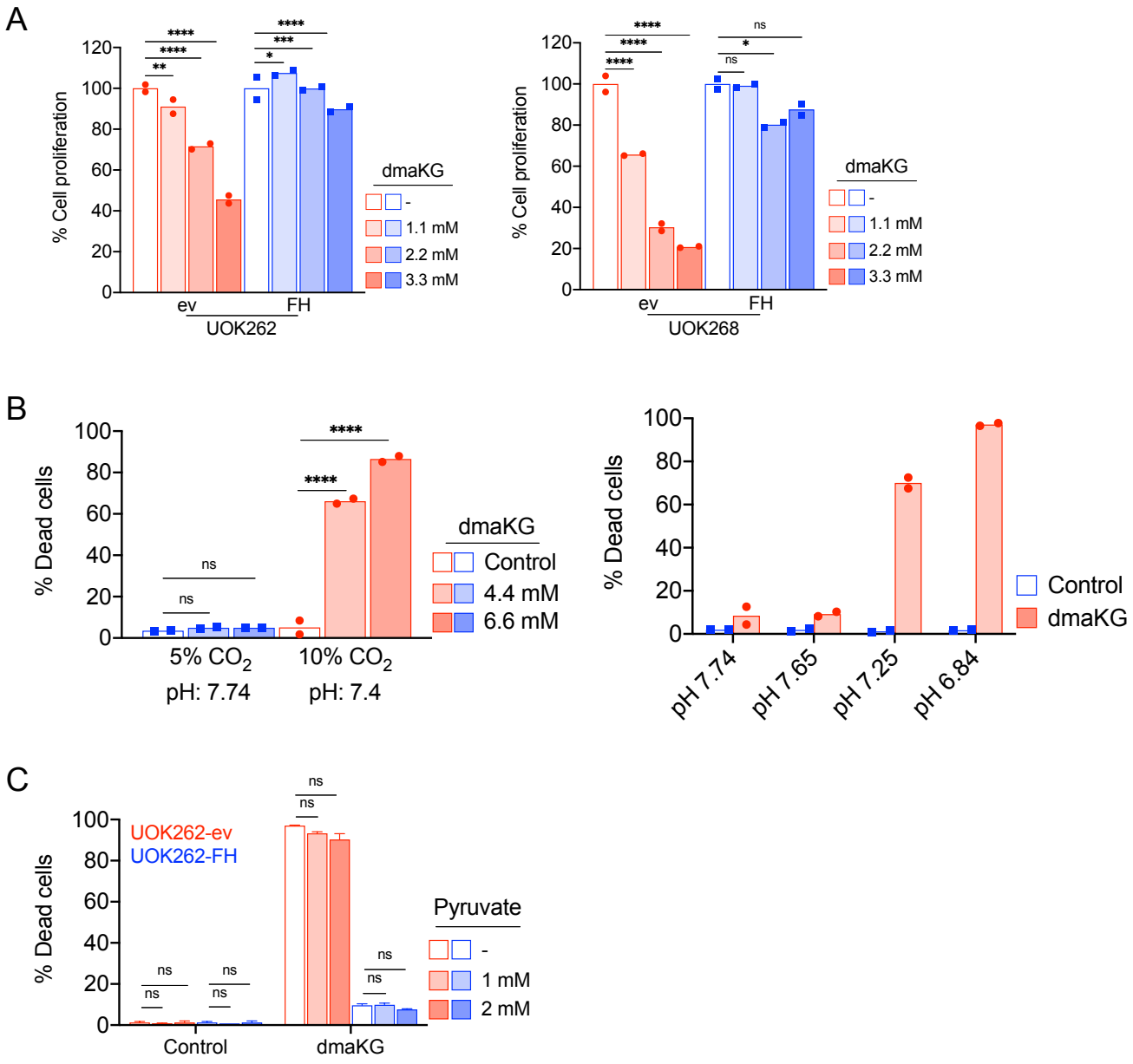

Figure S2. Antiproliferative effects of dmaKG and the effects of cell culture conditions on dmaKG sensitivity.

(A) Effects of long-term (4 days) dmaKG treatment on UOK262 (left panel) and UOK268 (right panel) cell pairs. % Cell proliferation is determined by crystal violet staining and calculated based on the respective control cells. Data are shown as mean and individual data points.

(B) Cytotoxicity studies with trypan blue exclusion assay to delineate the effect of media pH on dmaKG sensitivity in UOK262-ev cells. Unmodified DMEM growth medium is pH 7.74 in 5% CO_2 incubator and pH 7.4 in 10% CO_2 incubator (left panel). UOK262-ev cells in any media or CO_2 conditions at pH ≤ 7.4 are sensitive to dmaKG (both panels). Data are shown as mean and individual data points.

(C) Toxicity of dmaKG against the UOK262 cell pair. The concentration of pyruvate in the media is as indicated (mean ± SD, n = 2).

Statistical analyses were performed using two-way ANOVA with Tukey's multiple comparison (ns $P > 0.05$; *$P \leq 0.05$; **$P \leq 0.01$; ***$P \leq 0.001$; ****$P \leq 0.0001$). ev, empty vector; FH, FH-expression vector.

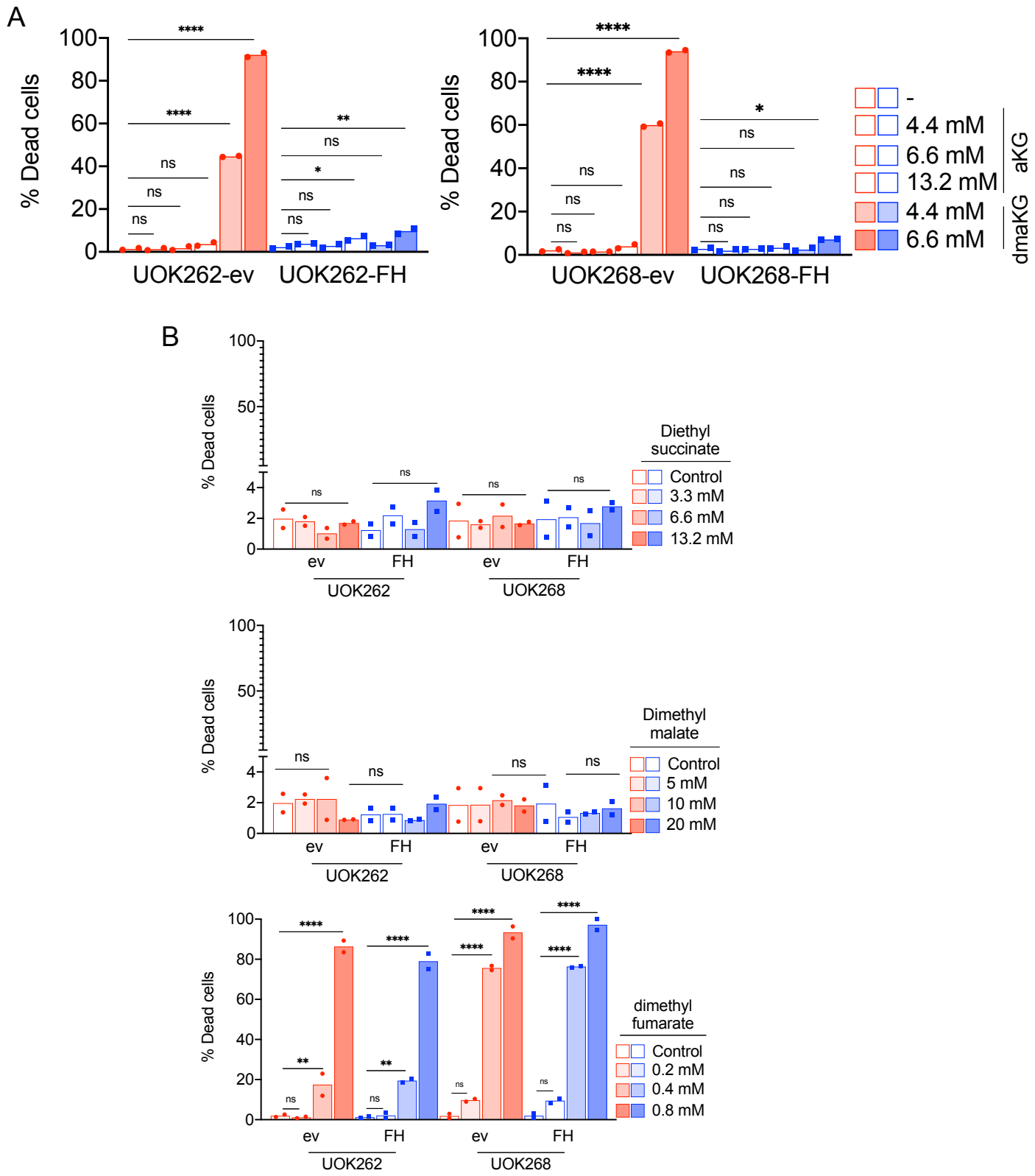

Figure S3. Cell-impermeable aKG and other cell-permeable Krebs cycle intermediates are not selectively toxic to the UOK262-ev cells.

(A) Cytotoxicity of dmaKG versus cell-impermeable alpha-ketoglutaric acid (aKG) in UOK262 and UOK268 cell pairs.

(B) Cytotoxicity of cell-permeable esters of Krebs cycle metabolites including diethyl succinate, dimethyl fumarate and dimethyl malate in UOK262 and UOK268 cell pairs.

Data are shown as mean and individual data points. Statistical analyses were performed using two-way ANOVA with Tukey's multiple comparison (ns $P > 0.05$; *$P \leq 0.05$; **$P \leq 0.01$; ***$P \leq 0.001$; ****$P \leq 0.0001$).

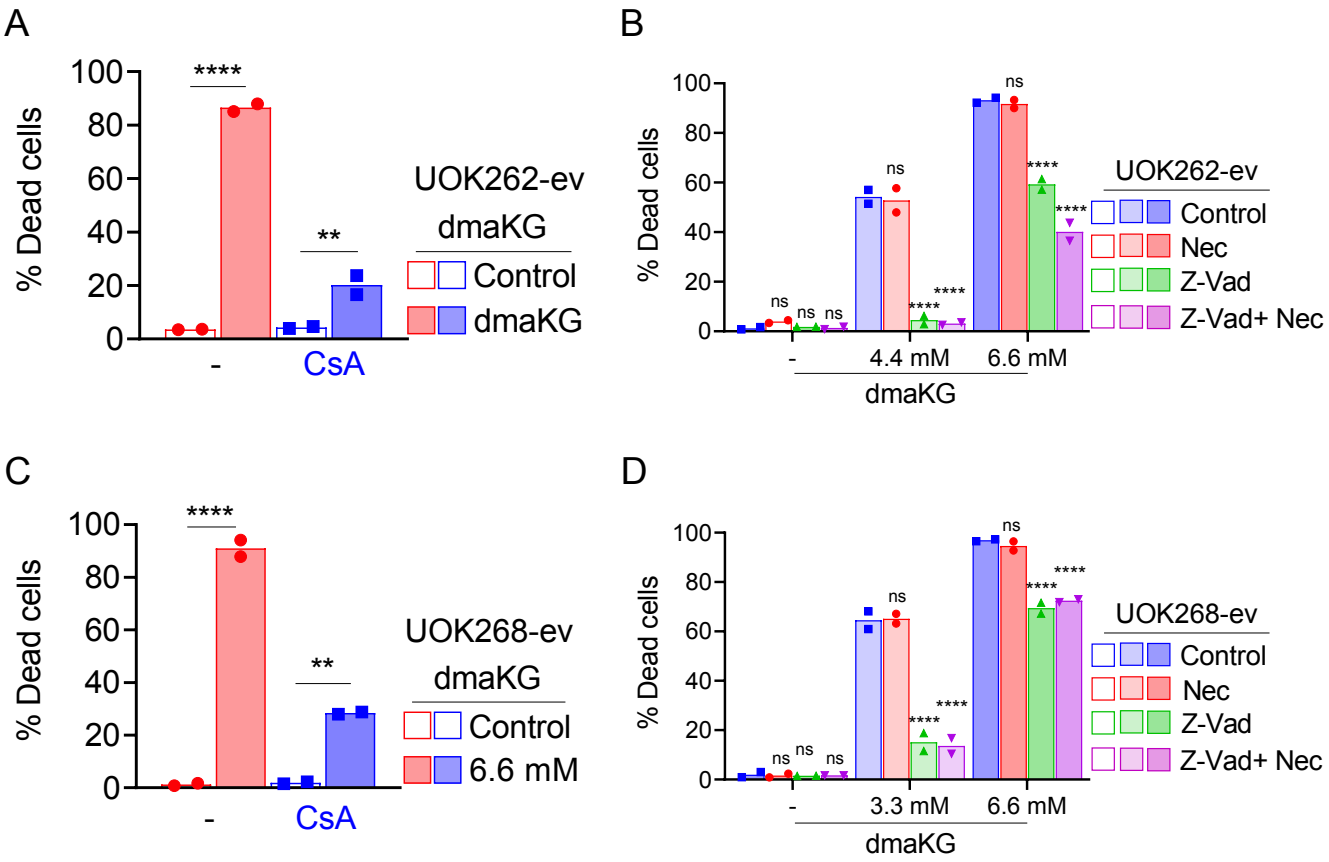

Figure S4. dmaKG induces a combination of mitochondria-mediated cell death mechanisms.

(A-B) Cytotoxicity analysis of HLRCC cells treated with the vehicle (Control) or dmaKG in the absence or presence of cyclosporine A (CsA). Cyclosporin A reduces the cytotoxicity induced by dmaKG in UOK262-ev and UOK268-ev cells. ev, empty vector.

(C-D) Cytotoxicity analysis of HLRCC cells evaluating the effects of cell death inhibitors pan-caspase inhibitor Z-VAD-FMK (Z-Vad) alone or in combination with necrostatin (Nec).

Data are shown as mean and individual data points. Statistical analyses were performed using two-way ANOVA with Tukey's multiple comparison (ns $P > 0.05$; *$P \leq 0.05$; **$P \leq 0.01$; ***$P \leq 0.001$; ****$P \leq 0.0001$).

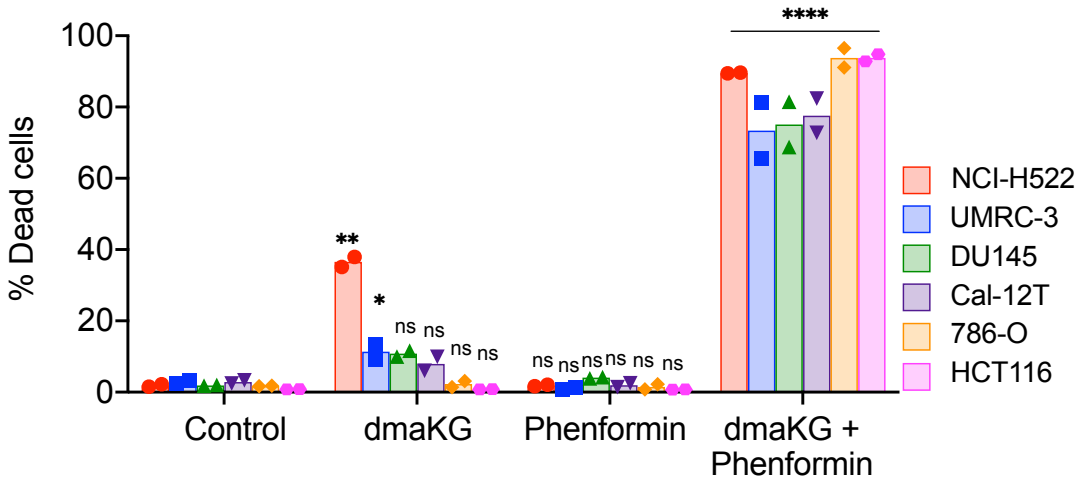

Figure S5. dmaKG is toxic to various cancer cell types in combination with phenformin.
Cytotoxicity of dmaKG in combination with ETC complex I inhibitor, phenformin (300 μM for DU145, 100 μM for all other cell lines). The concentrations of dmaKG are 3.3 mM for HCT116, 4.4 mM for NCI-H522, 6.6 mM for DU145, and 8.8 mM for UMRC-3, Cal-12T and 786-O. Data are shown as mean and individual data points. Statistical analyses were performed by two-way ANOVA with Tukey's multiple comparison using respective control of each cell types (ns $P > 0.05$; *$P \leq 0.05$; **$P \leq 0.01$; ***$P \leq 0.001$; ****$P \leq 0.0001$).

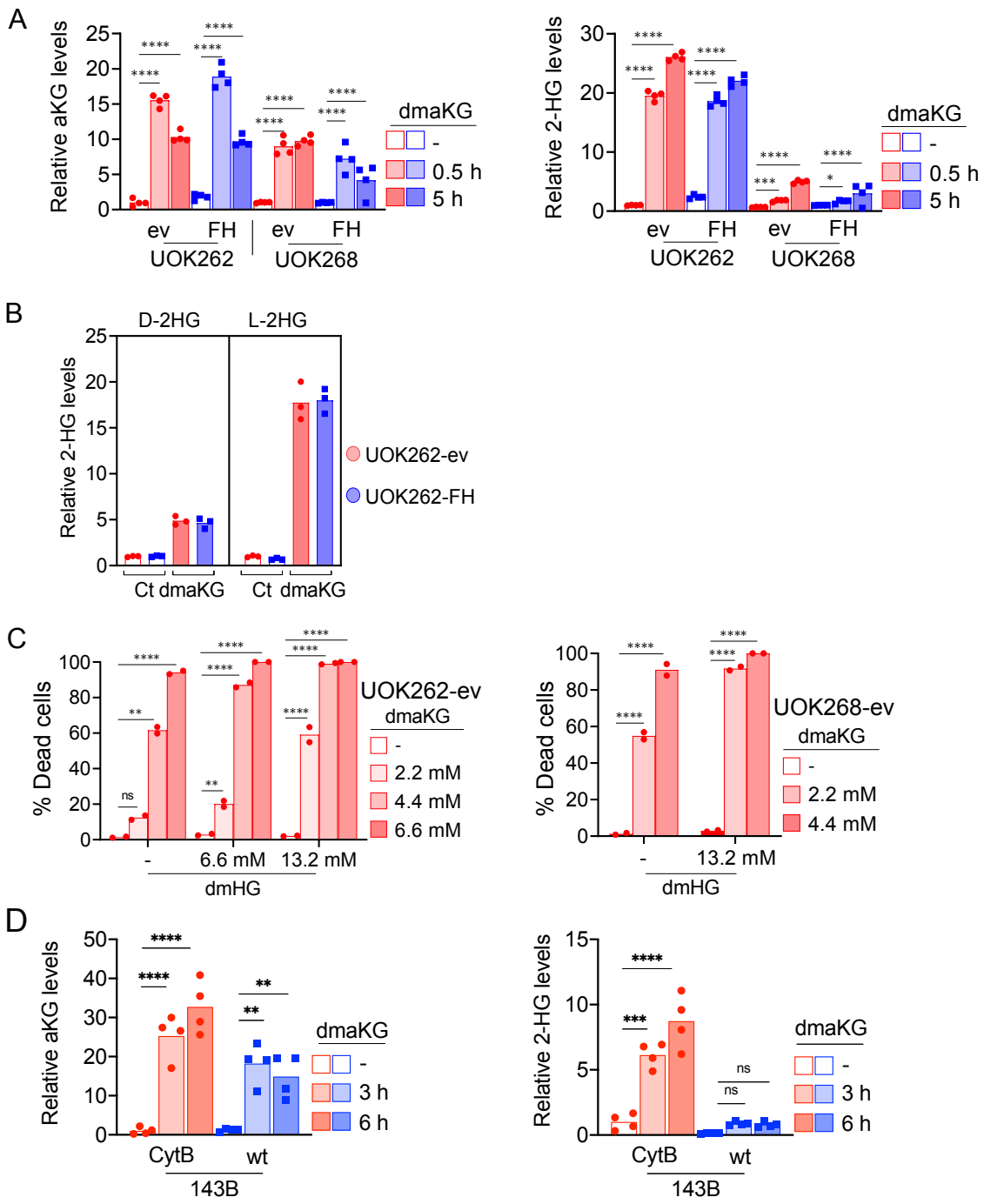

Figure S6. dmaKG treatment elevates intracellular aKG and 2-HG levels.

(A) Mass spectrometry analysis of UOK262 and UOK268 cell pairs indicating the relative abundance of alpha-ketoglutarate (aKG) (left panel) and 2-hydroxyglutarate (2-HG) (right panel) in control (-) or with 0.5 hr or 5-hr of dmaKG (6.6 mM) treatment.

(B) Chiral derivatization and GC-MS/MS analysis assessing the relative abundance of D-2HG and L-2HG in the UOK262 cell pair. Ct, control.

(C) Cytotoxicity analysis of dimethyl L-2HG (dmHG) alone or in combination with dmaKG. % Dead cells is measured by trypan blue staining after 24 hr of treatment.

(D) Mass spectrometry analysis of the 143B cell pair indicating the relative abundance of aKG (left panel) and 2-HG (right panel). Cells without treatment (-) or after 3 or 6 hr of dmaKG (9.9 mM) treatment were used.

Data are shown as mean and individual data points. Statistical analyses were performed using two-way ANOVA with Tukey's multiple comparison (ns $P > 0.05$; *$P \leq 0.05$; **$P \leq 0.01$; ***$P \leq 0.001$; ****$P \leq 0.0001$).

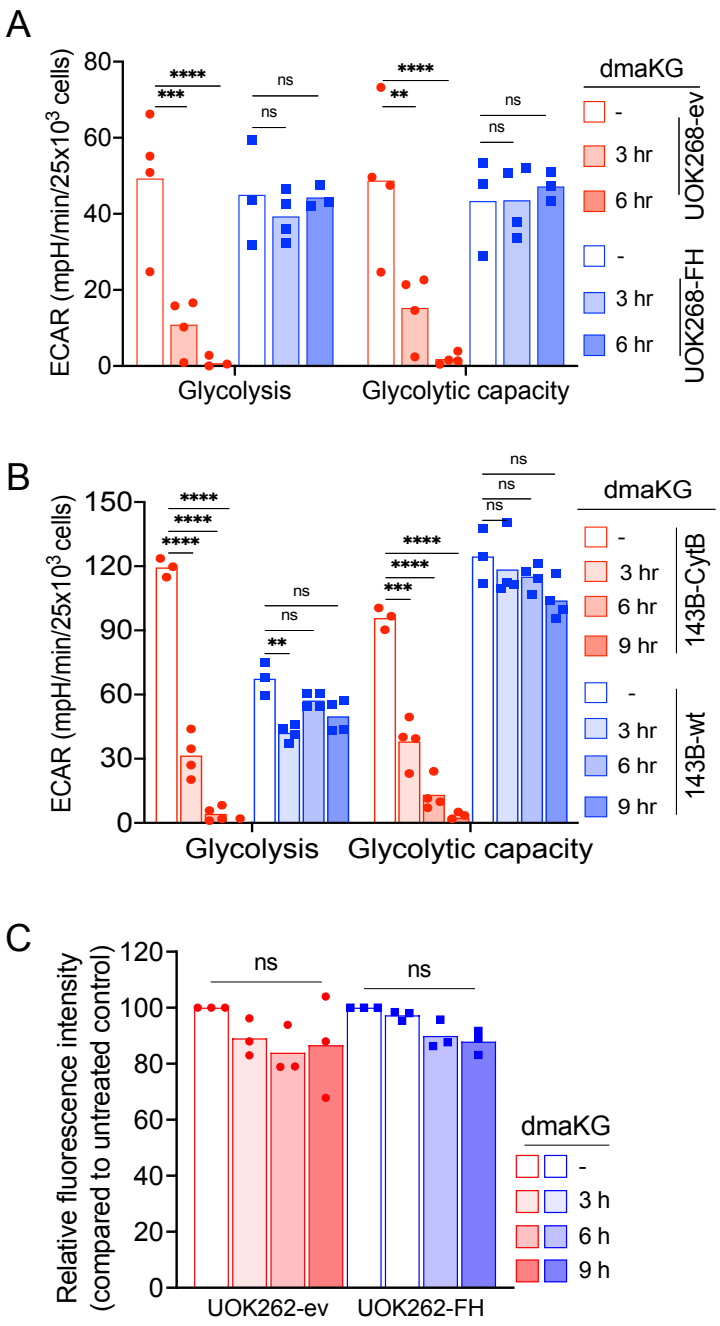

Figure S7. dmaKG selectively decreases glycolytic function in OXPHOS-incompetent cell condition.

(A-B) Glycolysis stress assay on UOK268 (A) and 143B (B) cell pairs. Data are shown as mean and individual data points. The extracellular acidification rate (ECAR) is used as a proxy for the outcome of glycolysis.

(C) Glucose transport as measured by 2-NBDG, a fluorescent glucose analog used to monitor glucose uptake, in the UOK262 cell pair. The bar graph shows the relative mean fluorescence intensity (MFI) of 2-NBDG. The data indicate that dmaKG (6.6 mM) did not alter the glucose uptake during the time when it reduced the ECAR in these cells (Fig. 2D).

Statistical analyses were performed using two-way ANOVA with Tukey's multiple comparison (ns $P > 0.05$; *$P \leq 0.05$; **$P \leq 0.01$; ***$P \leq 0.001$; ****$P \leq 0.0001$). ev, empty vector; FH, FH expression vector. .

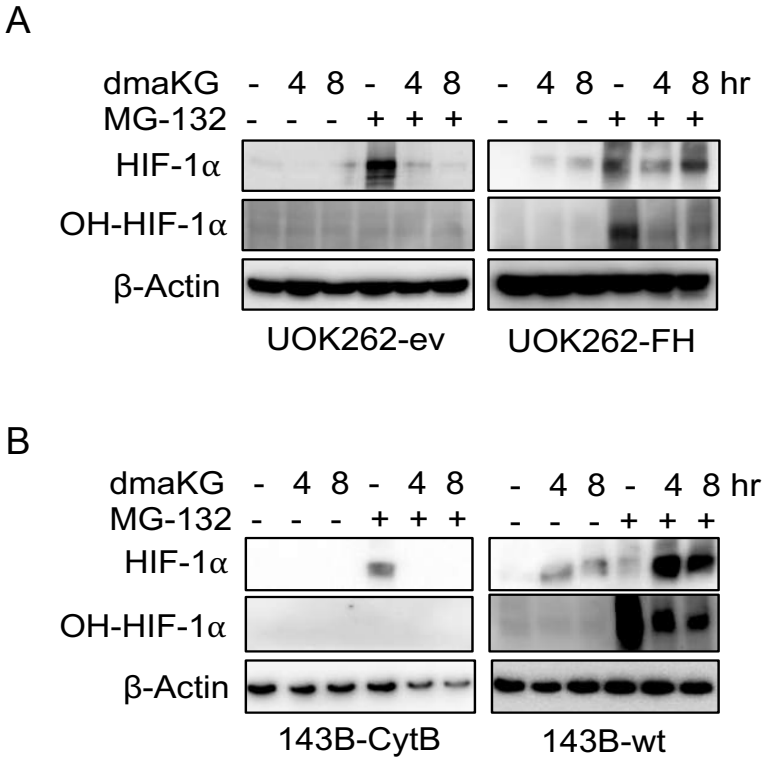

Figure S8. dmaKG decreases prolyl hydroxylation of HIF-1α.

Western blot analysis of UOK262 (A) and 143B (B) cell pairs treated with or without dmaKG (6.6 mM for UOK262-ev and UOK262-FH; 9.9 mM for 143B-CytB and 143B-wt) for the indicated time. A duplicate set of the samples were treated with MG-132 (10 μM) for the last 2 hr before the cells were harvested. Cell lysates were prepared and immunoblotting was performed with anti-HIF-1α and anti-prolylhydroxylated HIF-1α (OH-HIF-1α) antibodies. β-actin was used as loading control.

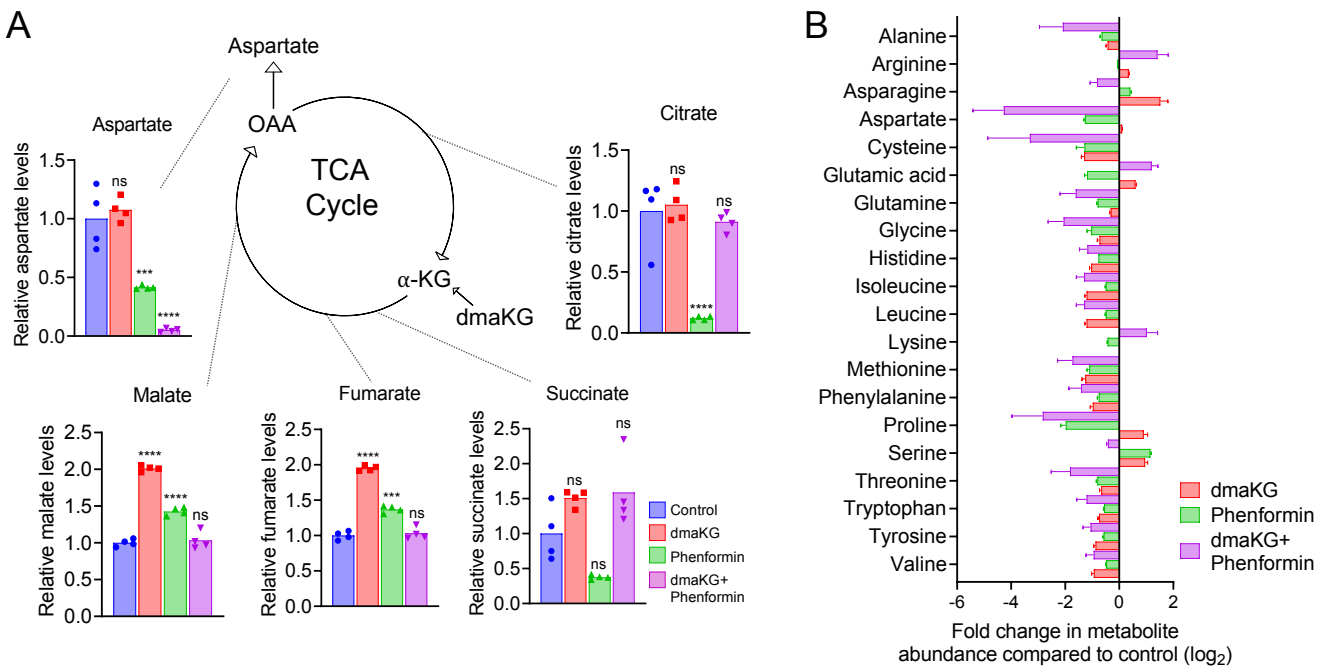

Figure S9. dmaKG and phenformin co-treatment depletes aspartate in 143B-wt cells.

(A) Mass spectrometry analysis of 143B-wt cells indicating the relative abundances of TCA cycle intermediates (citrate, succinate, fumarate, malate) and aspartate in control, dmaKG (9.9 mM, 6 hr), Phenformin (100 μM, overnight) and dmaKG + Phenfomrin (100 μM phenformin overnight and 9.9 mM dmaKG was added for the last 6 hr) samples. α-KG, alpha-ketoglutarate; OAA, oxaloacetate. Data are shown as mean and individual data points. Statistical analyses were performed using two-way ANOVA with Tukey's multiple comparison (ns $P > 0.05$; *$P \leq 0.05$; **$P \leq 0.01$; ***$P \leq 0.001$; ****$P \leq 0.0001$).

(B) The $\log_2$ fold changes of amino acids in 143B-wt cells after the indicated treatment as described above. Fold change was calculated relative to untreated control. Data are shown as mean ± SD.

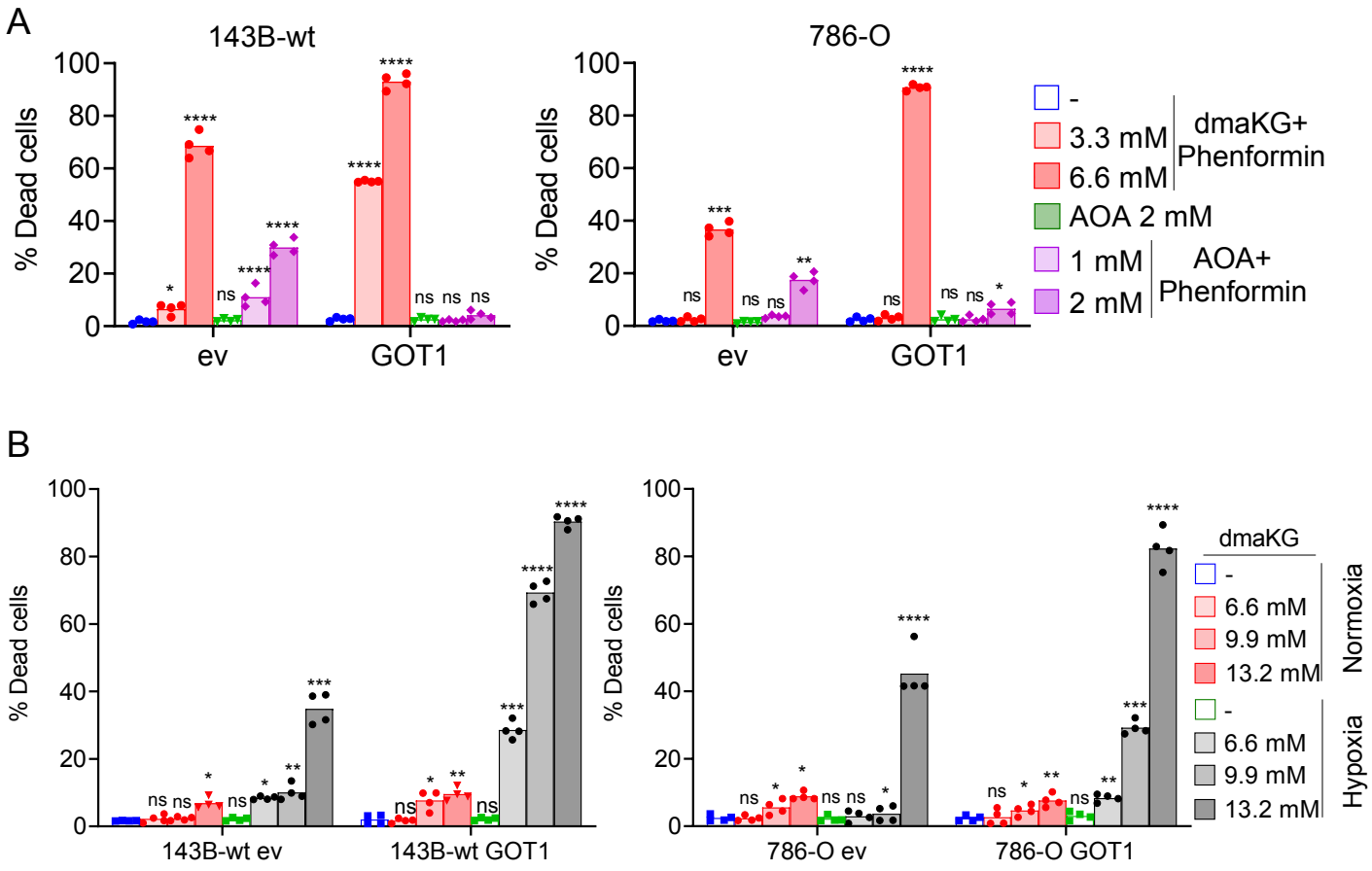

Figure S10. GOT1 overexpression sensitizes the cells to dmaKG in hypoxia or phenformin induced OXPHOS defects.

(A) Cytotoxicity studies with trypan blue exclusion assay. The data demonstrate that GOT1 overexpression enhances the toxicity of dmaKG and phenformin co-treatment but decreases the toxicity of AOA and phenformin co-treatment in 143B-wt (left panel) and 786-O (right panel) cells.

(B) Cytotoxicity analysis of cells treated in normoxia (21% O_2) or hypoxia (0.5% O_2). GOT1 overexpression in 143B-wt (left panel) and 786-O (right panel) sensitized them to dmaKG toxicity in hypoxia.

ev, empty vector; GOT1, GOT1-expression vector. Data are shown as mean and individual data points. Statistical analyses were performed using two-way ANOVA with Tukey's multiple comparisons (ns $P > 0.05$, *$P \leq 0.05$, **$P \leq 0.01$, ***$P \leq 0.001$, ****$P \leq 0.0001$).

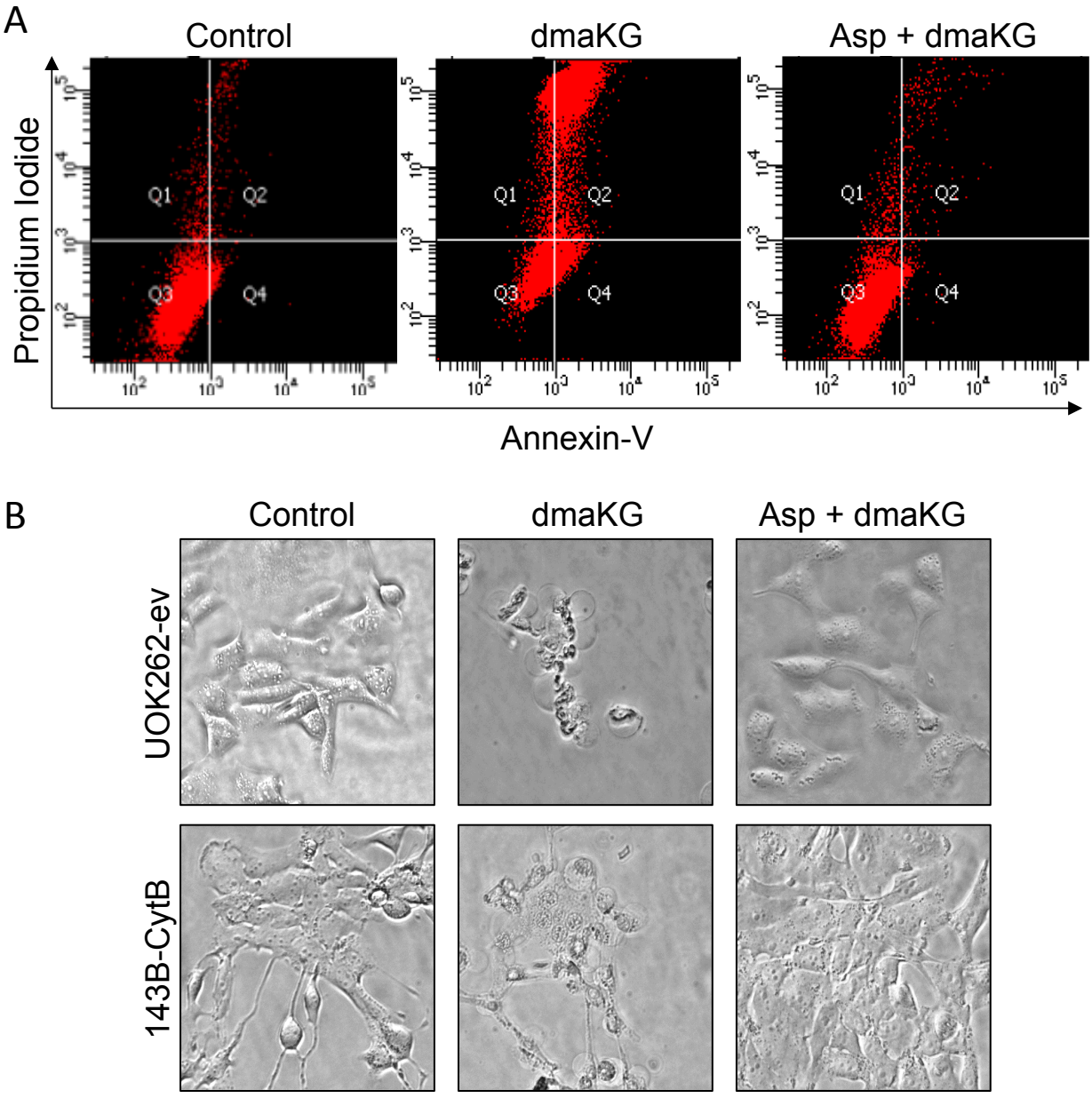

Figure S11. Aspartate supplementation reverses dmaKG-mediated cell death in OXPHOS-deficient cells. (A) Cytotoxicity studies by flow cytometric analysis following staining with FITC-conjugated annexin-V and propidium iodide (PI). UOK262-ev cells were treated with dmaKG (6.6 mM) in the absence or presence of aspartate (10 mM) for 22 hr.

(B) Phase contrast images of UOK262-ev and 143B-CytB cells treated with dmaKG (6.6 mM for UOK262-ev and 9.9 mM for 143B-CytB) in the absence or presence of aspartate (10 mM) for 22 hr.

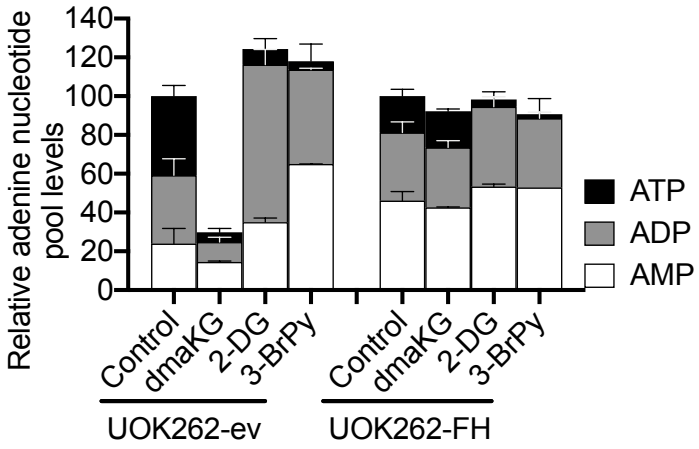

Figure S12. dmaKG causes adenylate depletion unlike other glycolysis inhibitors.
Measurement of the adenine nucleotide pool levels in UOK262 cell pairs after 6 hr of treatment with dmaKG (6.6 mM), 2-DG (20 mM), or 3-bromopyruvate (3-BrPy, 100 μM). dmaKG potently and selectively decreased AMP, ADP, and ATP levels in UOK262-ev (**P ≤ 0.01, ****P ≤ 0.0001, ****P ≤ 0.0001 respectively for AMP, ADP and ATP compared to untreated control) as compared to UOK262-FH (ns P > 0.05, ns P > 0.05, ns P > 0.05 respectively for AMP, ADP and ATP compared to untreated control), whereas 2-DG and 3-BrPy reduced ATP levels in both cell pairs (****P ≤ 0.0001, ****P ≤ 0.0001 in UOK262-ev and ***P ≤ 0.001, ****P ≤ 0.0001 in UOK262-FH) without causing significant changes in the overall adenine nucleotide pool levels (P = 0.0853, P = 0.3265 in UOK262-ev and P = 0.1081, P = 0.1328 in UOK262-FH). Data are shown as mean ± SD (n = 3, two-way ANOVA with Tukey's multiple comparisons).

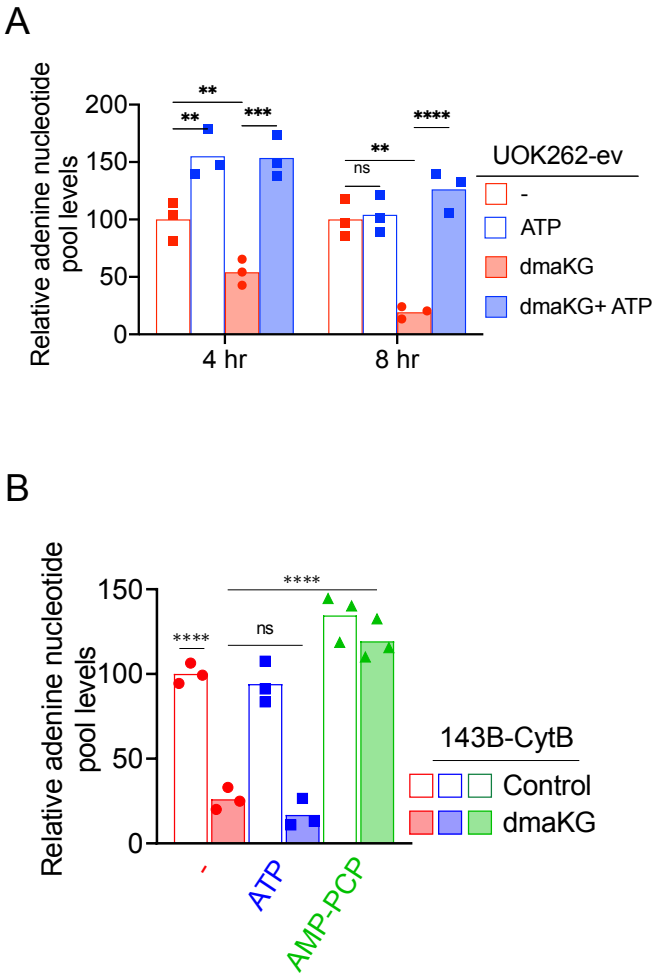

Figure S13. Exogenous supplementation of adenine nucleotides restores the adenine nucleotide pool levels in dmaKG-treated cells.

(A) Relative adenine nucleotide pool levels in UOK262-ev cells upon dmaKG treatment (6.6 mM) with or without ATP (1.2 mM) for 4 and 8 hr as indicated.

(B) Relative adenine nucleotide pool levels in 143B-CytB cells upon dmaKG treatment (9.9 mM) with or without ATP (1.2 mM) or AMP-PCP (100 μM) for 6 hr.

Data are shown as mean and individual data points. Statistical analyses were performed using two-way ANOVA with Tukey's multiple comparisons (ns $P > 0.05$, *$P \leq 0.05$, **$P \leq 0.01$, ***$P \leq 0.001$, ****$P \leq 0.0001$).

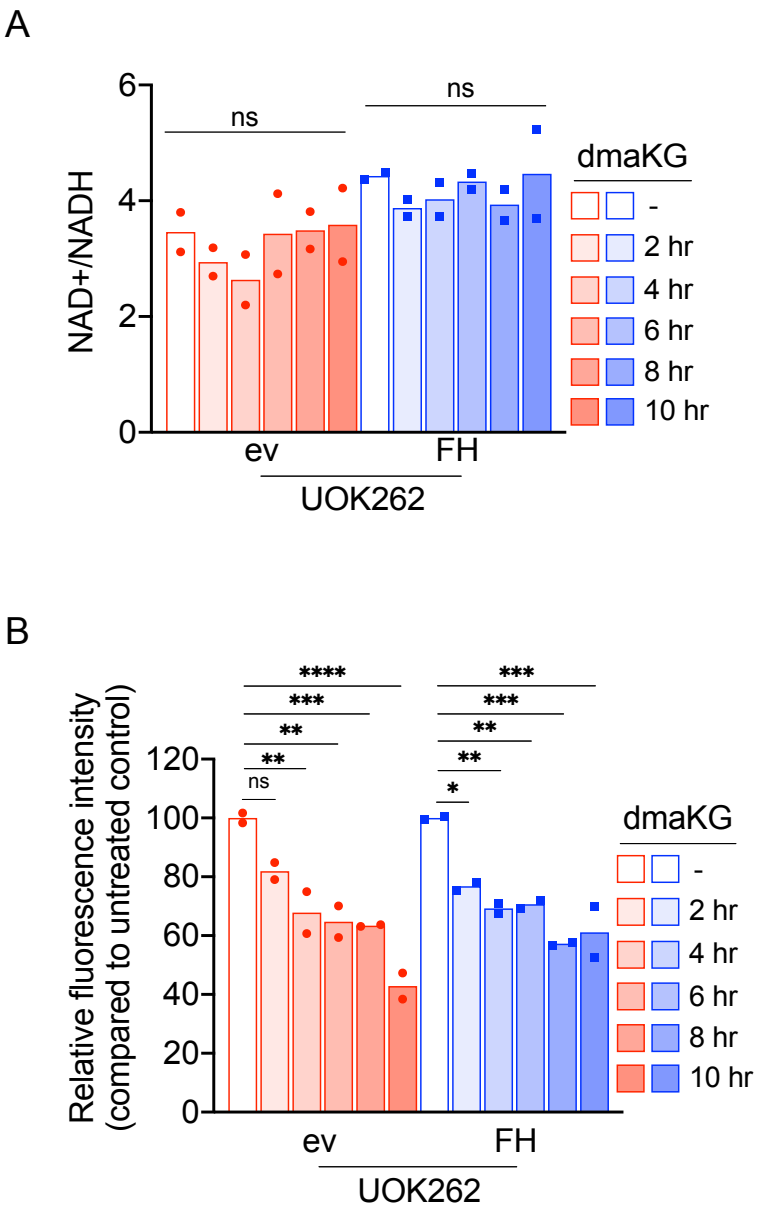

Figure S14. dmaKG does not alter the NAD+/NADH ratio but it depletes total NAD pool.
(A) Intracellular NAD+/NADH ratios and (B) relative NAD pool levels (including NAD+ and NADH) in UOK262 cell pair treated with dmaKG (6.6 mM) for the indicated lengths of time (two-way ANOVA with Tukey's multiple comparisons, ns $P > 0.05$; *$P \leq 0.05$; **$P \leq 0.01$; ***$P \leq 0.001$; ****$P \leq 0.0001$).

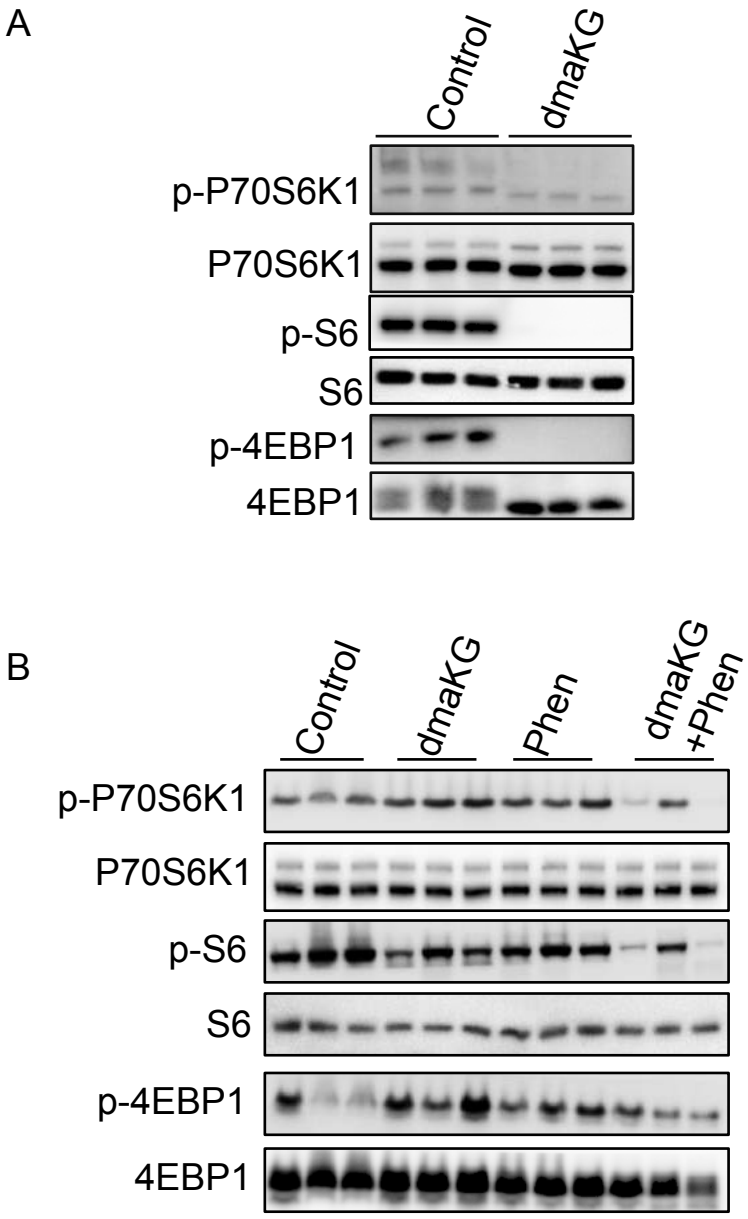

Figure S15. ***In vivo*** **administration of dmaKG suppresses mTOR pathway in tumors with mitochondrial dysfunction.**

Immunoblotting of proteins of mTOR pathway using lysates of 143B-CytB (A) and 143B-wt (B) tumors. dmaKG suppressed phosphorylation of P70S6K1, S6 and 4EBP1 in tumors with intrinsic OXPHOS deficiency (A) or phenformin-induced OXPHOS deficiency (B).

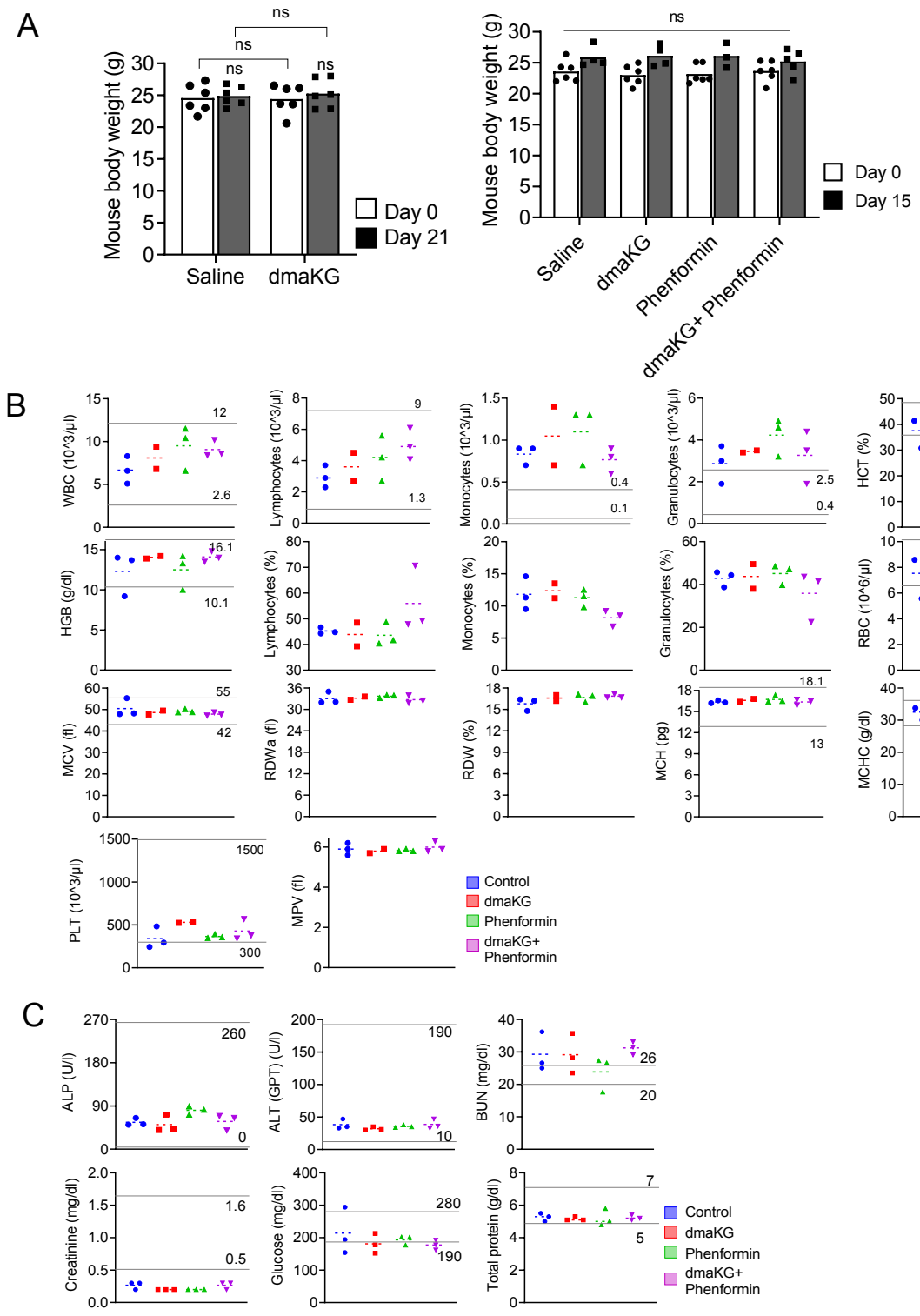

Figure S16. dmaKG is safe to the mice at the administered doses.

(A) Body weight of mice harboring 143B-CytB (left panel) or 143B-wt (right panel) tumors at the end of the experiments indicates no difference between saline and any of the other treatment groups (two-way ANOVA with Tukey's multiple comparisons, ns $P > 0.05$; *$P \leq 0.05$; **$P \leq 0.01$; ***$P \leq 0.001$; ****$P \leq 0.0001$).

(B) Blood count analysis on the final day of experiment on mice harboring 143B-wt xenograft tumors. No treatment conditions induced any significant changes in the various parameters tested as compared to the saline (Control) group. Most of the values were within the reference levels between two horizontal lines, suggesting no toxicity at the given dose and duration. No platelet clumps were present in any sample. Some parameters do not have known reference levels.

(C). Serum analysis of mice carrying 143B-wt xenograft tumors for various markers of hepatic and renal toxicities. No significant changes was observed as compared to the saline (Control) group. The reference ranges are indicated by two horizontal lines.

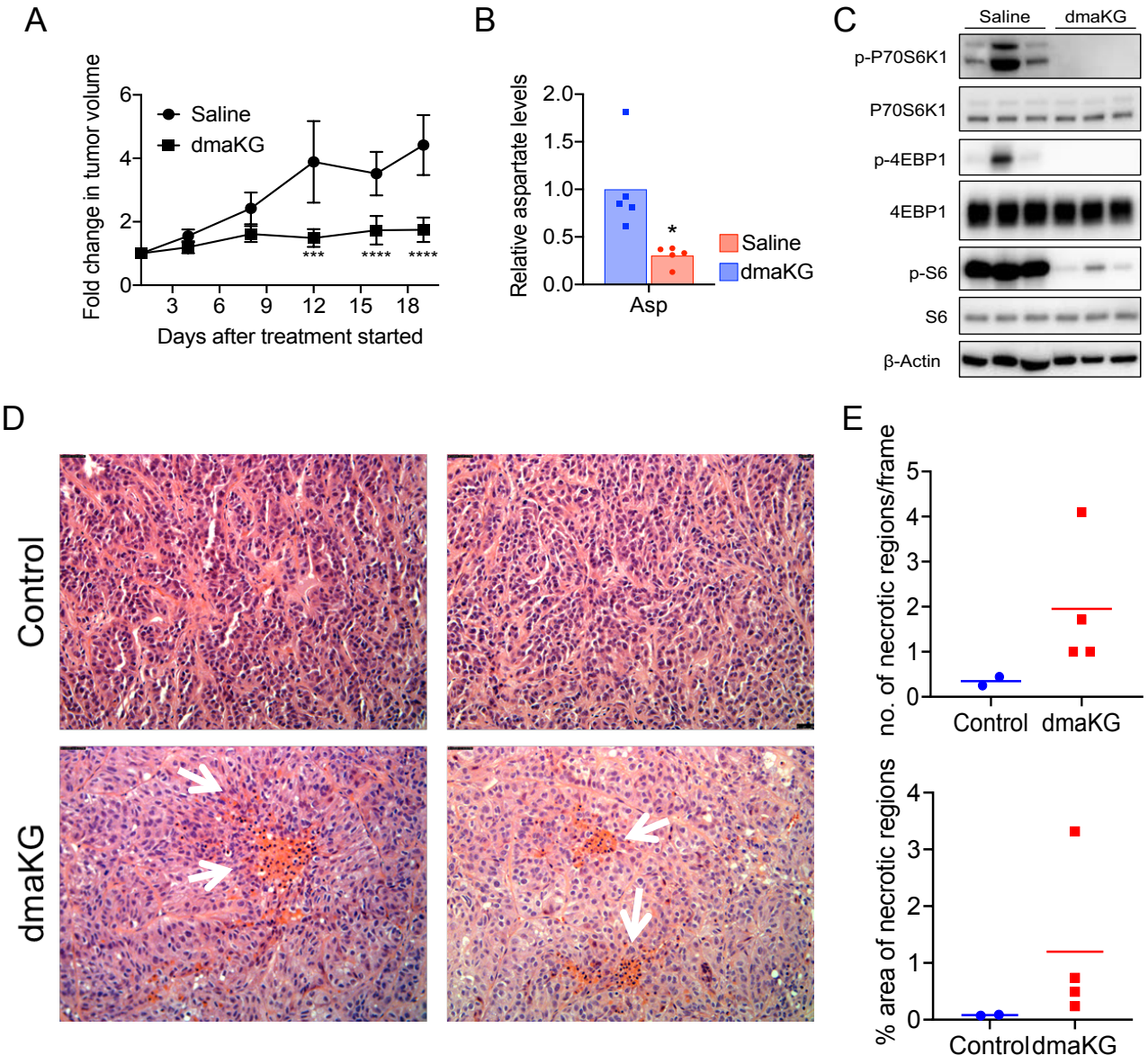

Figure S17. Antitumor effects of dmaKG on UOK262 xenograft tumor.

(A) Fold change in volume of the UOK262 xenograft tumor treated with saline or dmaKG (mean ± SD, n = 9, unpaired two-tailed t test with Welch's correction, *P ≤ 0.05; **P ≤ 0.01; ***P ≤ 0.001; ****P ≤ 0.0001).

(B) Mass spectrometry analysis of aspartate level in UOK262 tumor (unpaired two-tailed t test with Welch's correction, *P ≤ 0.05).

(C) Immunoblotting of components of mTOR signaling pathway and their phosphorylation using lysates prepared from three independent tumors each of the saline and the dmaKG groups.

(D) Examination of H&E-stained tumor sections identifies distinct regions of necrotic cells exhibiting pyknosis (nuclear condensation) and karyorrhexis (nuclear fragmentation) (white arrows) in dmaKG-injected, but not in saline-injected animals. Micrographs of two representative sections from each group are shown.

(E) Quantification of the average number of necrotic regions per image frame (top) and the percentage of area containing necrotic cells (bottom) from H&E-stained tumor sections. A necrotic region is defined as 5 or more cells exhibiting pyknosis and/or karyorrhexia. Data are shown for individual tumors. n=2, Control; n=4, dmaKG.

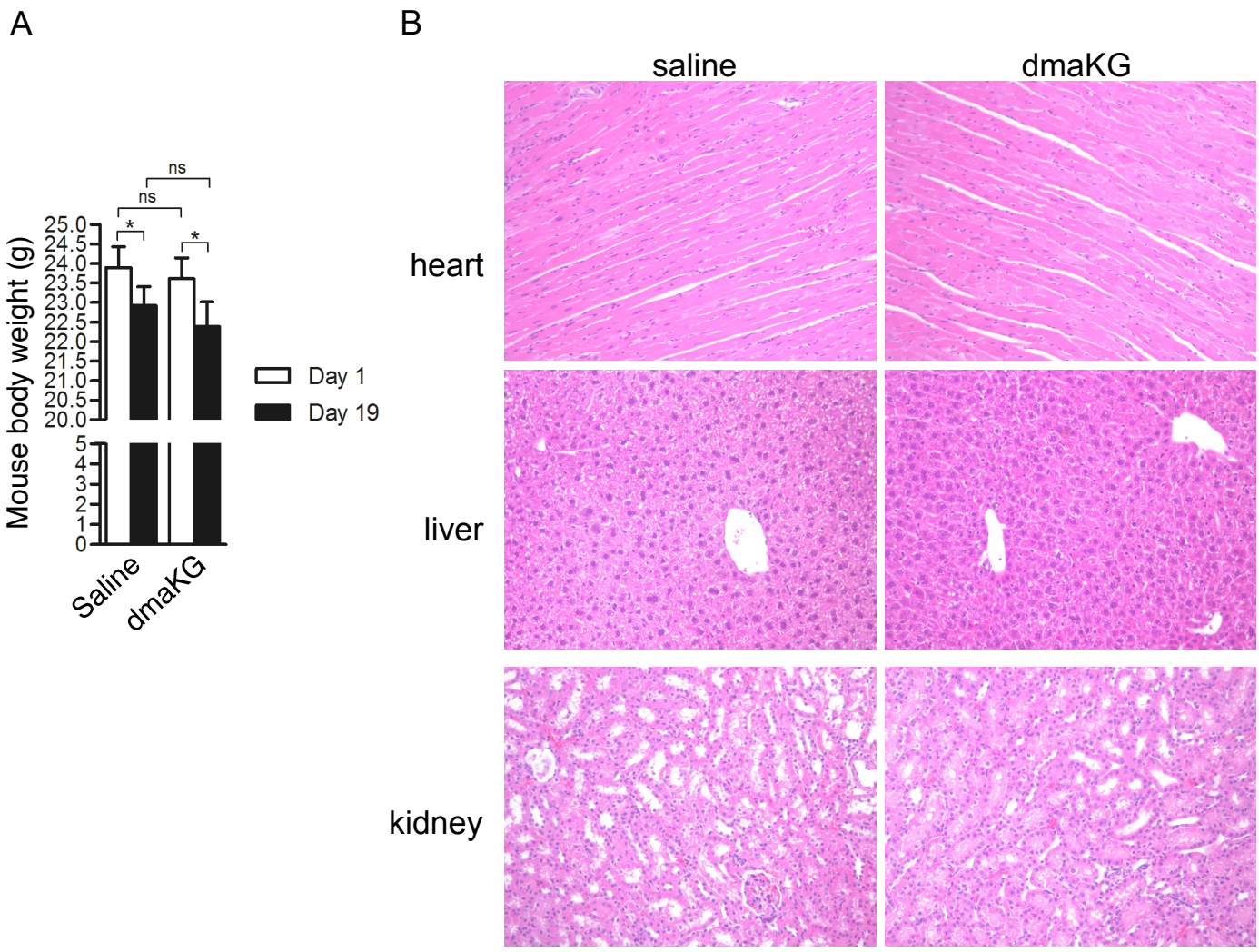

Figure S18. Administration of dmaKG does not cause detectable adverse effects in mice.

(A) Body weight of mice harboring UOK262 tumors and injected with saline or dmaKG. Both saline and dmaKG groups lost about 1 g of body weight over the course of treatment, which might be due to the bearing of the tumor and/or some stress caused by daily human handling. The weight changes were similar between two groups (average weight loss = 0.97 +/- 0.35 g for saline and 1.22 +/- 0.27 g for dmaKG, p = 0.57 by unpaired Student's t-test; n = 9 animals per group) suggesting no dmaKG-induced adverse effects.

(B) Sections (H&E staining) of heart, liver and kidney harvested from saline and dmaKG treated animals at the conclusion of the xenograft tumor experiment. No signs of tissue damage were found upon evaluation. Micrographs of a representative section for each group are shown.